Alkenone producers during late Oligocene-early Miocene revisited

Julien Plancq[a*], Vincent Grossi[a], Jorijntje Henderiks[b], Laurent Simon[c], Emanuela Mattioli[a]

[a] Laboratoire de Géologie de Lyon (UMR 5276), CNRS, Université Lyon 1, Ecole Normale Supérieure Lyon, Campus scientifique de la DOUA, Villeurbanne, France

[b] Uppsala University, Department of Earth Sciences, Paleobiology Program, Villavägen 16, 752 36 Uppsala, Sweden

[c] Laboratoire d'Ecologie des Hydrosystèmes Naturels et Anthropisés (UMR 5023), CNRS, Université Lyon 1, Campus scientifique de la DOUA, Villeurbanne, France

[*] Corresponding author : Laboratoire de Géologie de Lyon, UMR 5276, CNRS, Université Lyon 1, Campus de la DOUA, Bâtiment Géode, 69622 Villeurbanne Cedex, France. Tel.: +33 4 72431544.

E-mail address: julien.plancq@pepsmail.univ-lyon1.fr (J. Plancq)

This study investigates ancient alkenone producers among the late Oligocene-early Miocene coccolithophores recorded at Deep Sea Drilling Project Site 516. Contrary to common assumptions, *Reticulofenestra* was not the most important alkenone producer throughout the studied time interval. The comparison between coccolith species-specific absolute abundances and alkenone contents in the same sedimentary samples shows that *Cyclicargolithus* abundances explain 40% of the total variance of alkenone concentration and that the species *Cyclicargolithus floridanus* was a major alkenone producer, although other related taxa may have also contributed to the alkenone production at DSDP Site 516. The

distribution of the different alkenone isomers ($MeC_{37:2}$, $EtC_{38:2}$, and $MeC_{38:2}$) remained unchanged across distinct changes in species composition, suggesting similar di-unsaturated alkenone compositions within the Noelaerhabdaceae Family during the late Oligocene-early Miocene. However, the overall larger cell size of *Cyclicargolithus* may have implications for the alkenone-based reconstruction of past partial pressure of CO_2 (pCO_2). Our results underscore the importance of a careful evaluation of the most likely alkenone producers for periods (> 1.85 Ma) predating the first occurrence of contemporary alkenone-producers (i.e. *Emiliania huxleyi* and *Gephyrocapsa oceanica*).

1. Introduction

Alkenones are long-chain (C_{35}-C_{40}) lipids whose biosynthesis in modern oceans is restricted to a few extant unicellular haptophyte algae belonging to the Isochrysidales clade, which includes the calcifying haptophytes (coccolithophores) *Emiliania huxleyi* and *Gephyrocapsa oceanica* [*Marlowe et al.*, 1984; *Volkman et al.*, 1980, 1995]. A few non-calcifying Isochrysidales, such as *Isochrysis galbana*, also produce alkenones but they are restricted to coastal areas and are not considered as an important source of alkenone in the open ocean [*Marlowe et al.*, 1990].

Di- and tri-unsaturated C_{37} alkenones ($C_{37:2}$ and $C_{37:3}$ respectively) are ubiquitous and abundant in marine sediments, and have been intensively used for paleoceanographic reconstructions [e.g., *Brassell et al.*, 1986; *Jasper and Hayes*, 1990; *Eglinton et al.*, 1992; *Bard et al., 1997*; *Cacho et al.*, 1999; *Martrat et al.*, 2004; *Bolton et al.*, 2010]. The production of $C_{37:2}$ and $C_{37:3}$ alkenones is linked to the coccolithophore growth temperature [*Brassell et al.*, 1986; *Prahl and Wakeham*, 1987] and the so-called alkenone unsaturation index $U^{K'}_{37}$ (defined as the ratio $[C_{37:2}]/[C_{37:2}]+[C_{37:3}]$) has been used as a proxy to reconstruct past sea-surface temperatures, especially during the Quaternary period [e.g, *Müller et al.*,

1998; *Eltgroth et al.*, 2005; *Pahnke and Sachs*, 2006]. The carbon isotopic composition of the $C_{37:2}$ alkenone ($\delta^{13}C_{37:2}$) is also used to evaluate the carbon isotopic fractionation ($\varepsilon_{p37:2}$) that occurred during marine haptophyte photosynthesis in order to estimate concentration of CO_2 in past ocean surface waters ($[CO_{2(aq)}]$) and partial pressure of atmospheric CO_2 (paleo-pCO_2) [e.g., *Jasper and Hayes*, 1990; *Jasper et al.*, 1994; *Bidigare et al.*, 1997; *Pagani et al.*, 1999; *Pagani*, 2002; *Seki et al.*, 2010].

The alkenone-based proxies have been calibrated on modern coccolithophores in culture (*E. huxleyi* and *G. oceanica*) and on Quaternary sediments [e.g., *Conte et al.*, 1995, 1998; *Müller et al.*, 1998; *Popp et al.*, 1998; *Riebesell et al.*, 2000]. However, the temperature calibration of the $U^{K'}_{37}$ index is species-dependent [e.g., *Volkman et al.*, 1995; *Conte et al.*, 1998] and includes variability due to physiological factors such as nutrients and light availability [e.g., *Epstein et al.*, 1998; *Prahl et al.*, 2003]. Nutrient-limited chemostat cultures show that the carbon isotopic composition of alkenones and $\varepsilon_{p37:2}$ values vary with $[CO_{2(aq)}]$ and physiological factors such as growth rate (μ) and cell size [*Laws et al.*, 1995; *Popp et al.*, 1998]. However, nutrient-replete batch cultures produce much lower $\varepsilon_{p37:2}$ values and a different relationship between $\varepsilon_{p37:2}$ and μ / $[CO_{2(aq)}]$ [*Riebesell et al.*, 2000].

There is a huge gap between the first sedimentary record of alkenones in the Cretaceous at ~120 Ma [*Farrimond et al.*, 1986; *Brassell et al.*, 2004] and the first occurrence of modern alkenone producers (0.27 Ma for *E. huxleyi* [*Thierstein et al.*, 1977] and 1.85 Ma for *G. oceanica* [*Pujos-Lamy*, 1977]). Since *E. huxleyi* and *G. oceanica* cannot be responsible for alkenone production during most of the Cenozoic and the Mesozoic, the biological sources of alkenones preserved in pre-Quaternary sediments need to be elucidated in order to better constrain paleoenvironmental reconstructions based on these biomarkers.

Based on the consistent co-occurrence of *Reticulofenestra* coccoliths and alkenones in marine sediments dating back to the Eocene (45 Ma), *Marlowe et al.* [1990] suggested that the

most probable Cenozoic alkenone producers are to be found within the genus *Reticulofenestra*, which belongs to the Noelaerhabdaceae Family like *Emiliania* and *Gephyrocapsa*. However, this study did not compare alkenone concentrations with *Reticulofenestra* absolute abundances. More recently, *Bolton et al.* [2010] argued that *Reticulofenestra* species were the main alkenone producers during the late Pliocene, based on a correlation between *Reticulofenestra* abundances and C_{37} alkenone concentrations in sediments. Yet, other alkenones (e.g., C_{38}) were not considered.

Here, we investigate the co-occurrence of alkenones and coccolithophore genera and species during the late Oligocene-early Miocene by comparing nannofossil assemblages and species-specific absolute abundances with alkenone contents (C_{37} and C_{38} alkenones) in sediments from the Deep Sea Drilling Project (DSDP) Site 516. This allows a detailed characterization of ancient alkenone producers and a reappraisal of paleoceanographic and paleo-pCO_2 reconstructions for the investigated period.

2. Material and Methods

2.1. Sampling

DSDP Leg 72 Site 516 is located on the upper flanks of the Rio Grande Rise at 1313 m water depth in the South Atlantic subtropical gyre (Figure 1). Site 516 is situated north of the Northern Subtropical Front [*Belkin and Gordon*, 1996] and other front zones of the South Atlantic. During the Miocene, carbonate-rich sediments were deposited well-above the lysocline and the calcite compensation depth (CCD), at water depths similar to today [*Barker*, 1983]. Studies by *Pagani et al.* [2000a, 2000b] and *Henderiks and Pagani* [2007] demonstrated the simultaneous presence of Noelaerhabdaceae coccoliths and alkenones in DSDP Site 516 sediment samples. However, these studies neither reported alkenone

concentrations nor absolute abundances of coccoliths. We therefore selected a total of 35 sediment samples from Holes 516 and 516F. The sample depths slightly differ from those studied by *Henderiks and Pagani* [2007]. The time interval investigated spans the latest Oligocene and the early Miocene (25-16 Ma) and includes a period (~21–19 Ma) of major paleoceanographic changes [*Pagani et al.*, 2000b]. The age model for DSDP Site 516 used in this study is the one presented by *Henderiks and Pagani* [2007].

2.2. Total Organic Carbon (TOC) analyses

Sub-samples (ca. 100 mg of ground bulk sediment) were acidified *in-situ* with HCl 2N in pre-cleaned (combustion at 450°C) silver capsules until effervescence ceased, dried in an oven (50°C) and wrapped in tin foil before analyses. TOC analyses were performed with a Thermo FlashEA 1112 elemental analyzer using aspartic acid (36.09% of carbon) and nicotinamid (59.01% of carbon) as calibration standards (n=5 with variable weight for each standard). Accuracy was checked using in-house reference material analysed with the samples (fine ground low carbon sediment; 0.861 ± 0.034% of carbon (standard deviation; n=12)). All samples were analysed twice and the reproducibility achieved for duplicate analyses was better than 10% (coefficient of variation).

2.3. Alkenone analyses

Samples (ca. ~10g) were ground and extracted by way of sonication (5 x) using 50 mL of Dichloromethane (DCM)/Methanol (MeOH) (2:1 v/v). Following evaporation of the solvents, the total lipid extract was separated into three fractions using chromatography over a column of inactivated (4% H_2O) silica, with hexane (Hex), Hex/ethyl acetate (7:3 v/v) and DCM/MeOH (1:1 v/v) as eluents, respectively. The second fraction, containing alkenones, was dried under N_2, silylated (pyridine/N,O-bis(trimethylsilyl)trifluoroacetamide or BSTFA,

2:1 v/v, 60°C for 1h) and dissolved in hexane for analysis by gas chromatography (GC/FID) and gas chromatography/mass spectrometry (GC/MS).

Alkenones were identified by GC/MS using a MD800 Voyager spectrometer interfaced to an HP6890 gas chromatograph equipped with an on-column injector and a DB-5MS column (30 m x 0.25 mm x 0.25 μm). The oven temperature was programmed from 60°C (1 min) to 130°C at 20°C min^{-1}, and then to 310°C (20 min) at 4°C min^{-1}. Helium was used as the carrier gas at constant flow (1.1 mL min^{-1}).

Alkenone abundances were determined by GC/FID using hexatriacontane (*n*-C_{36} alkane) as internal standard. The GC was a HP-6890 Series gas chromatograph configured with an on-column injector and a HP5 (30 m x 0.32 mm x 0.25 μm) capillary column. Helium was used as the carrier gas at constant flow and the oven temperature program was the same as for GC-MS analyses. Samples were injected twice and the reproducibility achieved for duplicate alkenone quantifications was less than 10% (coefficient of variation).

2.4. Micropaleontological analyses

Slides for calcareous nannofossil quantitative analysis were prepared following the random settling method [*Beaufort*, 1991b; modified by *Geisen et al.*, 1999]. A small amount of dried sediment powder (5 mg) was mixed with water (with basic pH, over-saturated with respect to calcium carbonate) and the homogenized suspension was allowed to settle for 24 hours onto a cover slide. The slide was dried and mounted on a microscope slide with Rhodopass. Coccolith quantification was performed using a polarizing optical ZEISS microscope (magnification 1000x). A standard number of 500 calcareous nannofossils (coccoliths and nannoliths) were counted in a variable number (between 10 and 30) of field of views. In order to test the reproducibility of our quantification, each slide was counted twice and the reproducibility achieved was high (coefficient of variation: 10%).

151 Absolute abundance of nannofossils per gram of sediment was calculated using the
152 formula:

153 $$X = (N*V)/(M*A*H) \quad (1)$$

154 where X is the number of calcareous nannofossils per gram of sediment; N the number of
155 nannofossils counted in each sample; V the volume of water used for the dilution in the
156 settling device (mL); M the weight of powder used for the suspension (g); A the surface
157 considered for nannofossil counting (cm^2); H the height of the water over the cover slide in
158 the settling device (2.1 cm). Species-specific relative abundances (percentages) were also
159 calculated from the total nannofossil content.

160

161 Coccolith size is a proxy for cell size in ancient Noelaerhabdaceae [*Henderiks*, 2008].
162 *Henderiks and Pagani* [2007] have already evaluated the size variability within the
163 reticulofenestrids (namely species of the genera *Reticulofenestra* and *Dictyococcites*) at Site
164 516 and its implications for the interpretation of measured alkenone-based $\varepsilon_{p37:2}$ values. Here,
165 we pair the reticulofenestrid size data with the mean size variability of *Cyclicargolithus* in the
166 same 24 samples studied by *Henderiks and Pagani* [2007]. In each sample, 100 individual
167 *Cyclicargolithus* coccoliths were measured from four replicate slides, rendering statistically
168 robust estimates of mean size and its variance [*Henderiks and Törner*, 2006].

169

170 **2.5. Comparison between alkenone and nannofossil contents**

171 Our working hypothesis is that, under good preservation conditions, the alkenone
172 concentration should be related to the number of coccoliths of alkenone-producing taxa in
173 sediments. A similar assumption has already been used to identify biological sources of
174 alkenones in sediments of late Quaternary [e.g., *Müller et al.*, 1997; *Weaver et al.*, 1999] and
175 Pliocene age [e.g., *Bolton et al.*, 2010; *Beltran et al.*, 2011]. Here, we compare major trends of

absolute and relative abundances of coccolith genera to variations in total alkenone concentrations.

Simple and multiple linear regression analyses (significance threshold $\alpha = 0.05$) were used to determine the relationships between alkenone contents and relative/absolute abundances of coccolith genera, and between $\varepsilon_{p37:2}$ [data from *Pagani et al.*, 2000b], abundances of coccolith genera and mean sizes. The normality of the input data and residual distributions was checked using a Shapiro-Wilk test. All statistical analyses were performed using the JMP version 8.0.1 (SAS institute) software.

3. Taxonomy used for the Noelaerhabdaceae Family

Since the early publication of *Marlowe et al.* [1990], the genus *Reticulofenestra* has been considered by different authors as the most probable alkenone producer during the Cenozoic. However, species of the genus *Reticulofenestra* are generally considered to have a high morphological plasticity, and the *Dictyococcites* and *Cyclicargolithus* genera are often considered as junior synonyms of *Reticulofenestra* [e.g., *Theodoridis*, 1984; *Marlowe et al.*, 1990; *Young*, 1990; *Aubry*, 1992; *Beaufort*, 1992; *Henderiks and Pagani*, 2007; *Henderiks*, 2008]. Consequently, these genera have often been grouped either as reticulofenestrids [*Reticulofenestra* + *Dictyococcites;* e.g., *Henderiks and Pagani*, 2007; *Henderiks*, 2008] or more simply as *Reticulofenestra* [*Reticulofenestra* + *Dictyococcites* + *Cyclicargolithus*; e.g., *Aubry*, 1992]. This grouping can result in misleading conclusions when trying to precisely define ancient species involved in alkenone production. A taxonomic revision is beyond the scope of this work and *Dictyococcites*, *Reticulofenestra* and *Cyclicargolithus* are distinguished here on the basis of distinctive morphological features in optical microscope (Table 1 and taxonomic remarks).

4. Results

4.1. TOC

The studied samples are characterized by a low total organic carbon content (0.06% on average; Figure 2a). Higher values are recorded at the base of the studied interval and a slight trend to decreasing values is observed from 25 to 20 Ma, with a mean TOC content of 0.08% and 0.04 % before and after 20.5 Ma, respectively (Figure 2a).

4.2. Alkenones

One C_{37} and two C_{38} alkenones are present in all the samples studied. These were respectively identified as: heptatriacontadien-2-one ($MeC_{37:2}$), octatriacontadien-3-one ($EtC_{38:2}$) and octatriacontadien-2-one ($MeC_{38:2}$). $MeC_{37:2}$, $EtC_{38:2}$ and $MeC_{38:2}$ alkenones account for 55%, 33% and 12% of total alkenone content respectively and no significant variation of these proportions is observed through the time interval studied.

The total amount of these ketones is relatively low (0.03 µg g of sediment^{-1} on average), with a maximum of 0.13 µg g of sediment^{-1} at about 23 Ma (Figure 2b), and values attaining the detection limit at around 20 and 17 Ma. A general trend to decreasing alkenone content is seen from 25 to 16 Ma but three periods of increasing total alkenone content are observed at about 23, 22-21.5 and 19.5-17.5 Ma (Figure 2b). This overall distribution matches with that of TOC (Figure 2a and b). The same variations are observed when each alkenone is considered individually. Similar trends also occur when alkenone content is expressed relative to TOC (Figure 2c). In Figure 3, quantitative alkenone data expressed per gram of sediment are compared to absolute and relative abundances of Noelaerhabdaceae coccoliths.

4.3. Coccolith assemblages

226 Coccoliths are well preserved in all investigated samples since delicate coccoliths that are
227 prone to dissolution, such as *Syracosphaera* and *Pontosphaera*, are commonly observed with
228 pristine structures. This indicates that coccolith assemblages are not importantly biased by
229 selective dissolution in the water column or diagenetic effects, in agreement with previous
230 studies at Site 516 [*Henderiks and Pagani*, 2007].

231 The mean absolute abundance of nannofossils is 5.0×10^9 nannofossils g of sediment^{-1} and
232 does not show any significant stratigraphic trend across the late Oligocene-early Miocene
233 (Figure 2d). Coccolith assemblages are dominated by four genera, which account for 70-80%
234 of the total assemblage, namely: *Reticulofenestra*, *Dictyococcites*, *Cyclicargolithus*, all
235 belonging to the Noelaerhabdaceae Family, and *Coccolithus*. No significant stratigraphic
236 trend across the late Oligocene-early Miocene is observed when all the Noelaerhabdaceae are
237 combined (Figure 2e). The mean absolute abundance of Noelaerhabdaceae is 3.4×10^9
238 coccoliths g of sediment^{-1} (Figure 2e).

239 For each genus of Noelaerhabdaceae, relative and absolute abundances show similar
240 variations through time (Figure 3b, c and d). Three shifts in coccolith assemblages can be
241 distinguished: (1) Between 25 and 20.5 Ma, coccolith assemblages are dominated by
242 *Cyclicargolithus* representing on average 30% (1.4×10^9 specimens g of sediment^{-1}) of the total
243 nannofossil assemblage, whereas *Dictyococcites* represents ca. 25% (1.3×10^9) and
244 *Reticulofenestra* ca. 15% (0.7×10^9); (2) between 20.5 and 17.5 Ma, coccolith assemblages
245 show a dominance of *Dictyococcites* (40%; 2.3×10^9) and an increase (from 15% to 45%;
246 0.95×10^9 to 2.0×10^9) in the proportion of *Reticulofenestra*, whereas *Cyclicargolithus* shows a
247 sharp decrease in abundance (8%; 0.42×10^9); (3) assemblages between 17.5 and 16 Ma are
248 characterized by the dominance of *Reticulofenestra* (45%; 2.0×10^9) with smaller amounts of
249 both *Cyclicargolithus* (9%; 0.44×10^9) and *Dictyococcites* (8%; 0.42×10^9). In general,
250 *Dictyococcites* and *Cyclicargolithus* abundances show opposite trends (Figure 3b and c). This

record is consistent with the results of *Henderiks and Pagani* [2007] although the apparent timing in assemblage shifts is slightly different due to different sample spacing.

The coccolith size of *Cyclicargolithus*, which is strongly linearly correlated to its cell diameter [*Henderiks*, 2008], ranges between 4-12 μm (N=2454). Mean size per sample varies between 6.13 μm ± 0.24 (95% confidence mean) in the late Oligocene and 8.45 μm ± 0.18 (95% conf. mean) in the early Miocene.

5. Discussion

5.1. Alkenone producers at DSDP Site 516

Significant correlations between the abundance of coccoliths of the main alkone-producers (namely *E. huxleyi* and *G. oceanica*) and the alkenone concentration have been observed in late Quaternary sediments [e.g., *Müller et al.*, 1997; *Weaver et al.*, 1999]. Based on this observation, parallel distributions of reticulofenestrid coccoliths and alkenone contents have been used to identify past biological sources of alkenones in Pliocene sediments [e.g., *Bolton et al.*, 2010; *Beltran et al.*, 2011]. The similar variations at DSDP Site 516 between the absolute abundance of *Cyclicargolithus* coccoliths and the total alkenone content (Figure 3) suggests a significant contribution of this genus to alkenone production between 25 and 16 Ma. More precisely, alkenone production is supported by the species *C. floridanus* which is entirely responsible for the *Cyclicargolithus* abundance trend (Figure 4). Although reticulofenestrids are sometimes considered as species having high morphological plasticity which may bias their taxonomy [e.g., *Beaufort*, 1991a], *C. floridanus* represents a very characteristic morphospecies easily distinguishable from other reticulofenestrids due to its larger size and distinct sub-circular shape.

Processes of degradation in the water column and in sediments may affect alkenone and coccolith records differently, leading to misleading interpretations of the sedimentary record. In the present case, several observations argue against the effects of such potential preservation biases.

First, records of coccolith assemblages can be skewed by the dissolution of susceptible species during settling and sedimentary burial [*Roth and Coulbourn*, 1982; *Gibbs et al.*, 2004; *Young et al.*, 2005]. Such selective coccolith dissolution is not observed within the studied nannofossil groups at DSDP Site 516 [*Henderiks and Pagani*, 2007; this study]. Sediments from Site 516 are calcareous oozes with little evidence of dissolution or cementation precipitation [*Barker et al.*, 1983], and no significant secondary calcite overgrowth is observed on coccoliths [*Ennyu et al.*, 2002]. An important effect of diagenesis affecting the recorded coccolith assemblages can thus be excluded.

Second, a majority of organic matter produced in the surface oceans is generally remineralized before and after reaching the seafloor. The concentrations of TOC and alkenones in sediments are thus a function of preservation conditions and represent only a fraction of the original export productivity. Nevertheless, the relatively high sedimentation rate (17 m/Ma) and the relatively shallow water depth (1313 m) of DSDP Site 516 [*Barker et al.*, 1983] induced a limited oxidation and a relatively rapid burial of organic matter into the sediments compared to other oceanic settings [*Mukhopadhyay et al.*, 1983]. Moreover, the paleo-depth of the studied site did not change significantly during the time span investigated. Changes in TOC and alkenone concentrations in sediments may also reflect varying sedimentation rate. However, the sedimentation rate calculated according to the age model of the studied interval does not show significant variations [*Pagani et al.*, 2000b; *Henderiks and Pagani*, 2007]. Thus the observed overall decrease in TOC since ~21.5 Ma (Figure 2a) likely reflects a decrease in primary productivity in response to paleoceanographic changes (mainly

300 linked to temperature and nutrient concentrations; *Pagani et al.*, 2000b; *Henderiks and*
301 *Pagani*, 2007) rather than changes in sedimentary dilution or organic matter degradation.
302 Despite the fact that alkenones represent only a very small fraction of TOC, the significant co-
303 variation observed between TOC and total alkenone content (Figure 2a and b; R^2= 0.69,
304 p<0.0001) suggests that alkenone distribution also reflects variations in the abundance of
305 alkenone producers rather than an erratic degradation of alkenones relative to TOC. It should
306 be noted that these biolipids are generally considered less prone to degradation than other
307 phytoplankton-derived lipids [*Sun and Wakeham*, 1994; *Gong and Hollander*, 1997, 1999]. In
308 addition, the association between organic matter and the calcium carbonate of coccoliths
309 might have produced a physical and chemical protection against remineralization [*Armstrong*
310 *et al.*, 2002], as coccoliths have very likely acted as ballast and reduced the residence time of
311 organic matter within the water column [*Klaas and Archer*, 2002].

312 Finally, the apparent similar variations between the abundance of *Cyclicargolithus* and the
313 total alkenone content are supported by statistical analyses which show that, among all tested
314 Noelaerhabdaceae genera, only absolute and relative abundances of this genus produce
315 significant and positive linear correlations with the total alkenone content (R^2=0.36-0.44,
316 p<0.0005; Figure 5). Such a correlation is unlikely the result of diagenetic processes. Still, it
317 is possible that a better preservation of the calcite of coccoliths compared to alkenones has led
318 to an underestimation of the contribution of *Cyclicargolithus* to alkenone production. This
319 may partly explain why *Cyclicargolithus* represents only 40% of the total variance of
320 alkenone concentration. However, other taxa may have also contributed to the alkenone
321 production at DSDP Site 516 since *Cyclicargolithus* has a limited stratigraphical range (from
322 ~40 Ma to ~13 Ma; *Young*, 1998). The continuous co-occurrence of the *Reticulofenestra*
323 genus and alkenones throughout the Cenozoic sediment record is the main argument to infer it
324 is the most probable ancient alkenone producer [e.g., *Marlowe et al.*, 1990]. In the present

study, the quantitative distribution of *Reticulofenestra* shows an inverse trend compared to that of alkenone concentrations (Figure 3a and d). Moreover, when considering *Reticulofenestra* plus *Cyclicargolithus* abundances in a multiple linear regression calculated *versus* alkenone concentrations, the fit does not increase (R^2= 0.45, p<0.001) with respect to *Cyclicargolithus* alone (R^2=0.44, p<0.0005). These observations suggest a weak contribution of the genus *Reticulofenestra* to alkenone production in the time interval considered, although a contribution of this genus cannot be completely excluded. Abundances of *Dictyoccocites* (Figure 3c) do not significantly correlate either with the general trend of alkenone concentrations. However, a contribution of *Dictyococcites* to alkenone production cannot be excluded especially after 20.5 Ma where a small increase in alkenone content coincides with a sharp increase in *Dictyococcites* (Figure 3a and c). It is also possible that non-calcifying haptophytes, for which there is no mineralized fossil record, have contributed to the alkenone production at DSDP Site 516 although extant non-calcifying alkenone producers (e.g., *Isochrysis galbana*) are not considered as an important source of alkenones in modern open-ocean sediments [*Marlowe et al.*, 1990].

It is worth noticing that no change in the proportion of the different alkenone isomers ($MeC_{37:2}$, $EtC_{38:2}$, and $MeC_{38:2}$) is observed throughout the entire time interval considered in this study. This may imply that all alkenone-producing species produced the same type of alkenones during the late Oligocene-Early Miocene, which may not be surprising since the alkenone compositions of modern coccolithophorids (essentially *G. oceanica* and *E. huxleyi*) are rather similar [*Volkman et al.*, 1995]. It is possible, however, that the original distribution of alkenones at DSDP Site 516 contained alkenone isomers with more than two unsaturations, since tri- and tetra-unsaturated alkenones are known to be far more reactive towards

349 diagenetic processes than their di-unsaturated homologues [e.g., *Grimalt et al.*, 2000; *Rontani*
350 *and Wakeham*, 2008].
351
352 **5.2. Paleoenvironmental implications**
353 Past atmospheric CO_2 concentrations (pCO_2) can be estimated from the carbon isotopic
354 fractionation between ambient CO_2 and the algal cell ($\varepsilon_{p37:2}$) that occurred during marine
355 haptophyte photosynthesis [*Jasper and Hayes*, 1990; *Jasper et al.*, 1994; *Bidigare et al.*,
356 1997; *Pagani et al.*, 1999], based on the expression:
357 $$\varepsilon_{p37:2} = \varepsilon_f - b/[CO_{2(aq)}] \quad (2)$$
358 where $\varepsilon_{p37:2}$ is calculated from the difference between the carbon isotopic compositions of
359 di-unsturated C_{37} alkenone ($\delta^{13}C_{37:2}$) and foraminifera carbonate ($\delta^{13}C_{foram}$) [for further details
360 see *Pagani et al.*, 1999]. ε_f is the carbon isotope fractionation due to all carbon-fixing
361 reactions (here assuming ε_f = 25‰ [*Popp et al.*, 1998]) and '*b*' represents the sum of
362 physiological factors, including growth rate and cell geometry, that affect total carbon isotope
363 discrimination [*Laws et al.*, 1995; *Popp et al.*, 1998]. The magnitude of term '*b*' is estimated
364 by the phosphate concentration of the surface ocean [*Bidigare et al.*, 1997; *Pagani et al.*,
365 1999]. In oligotrophic settings, it is generally assumed that the influence of haptophyte growth
366 rates on $\varepsilon_{p37:2}$ is negligible [e.g., *Pagani et al*., 2005].
367 Considering that larger phytoplankton cells, with higher carbon cell quota relative to
368 surface area, fractionate less than smaller cells under similar $CO_{2(aq)}$ and low growth rates
369 [e.g. *Laws et al.*, 1995; *Popp et al.*, 1998], *Henderiks and Pagani* [2007] applied a cell-size
370 correction to the term '*b*' in order to revise pCO_2 trends reconstructed by *Pagani et al.* [2000b]
371 at DSDP Site 516. This correction was based on the cell diameter of reticulofenestrids,
372 namely *Reticulofenestra* and *Dictyococcites*, considered as the most probable alkenone
373 producers during the Cenozoic. Indeed, a significant correlation exists between alkenone

374 $\delta^{13}C_{37:2}$ (and therefore $\varepsilon_{p37:2}$) and reticulofenestrid mean size (R=0.68, *p*=0.0003; Table 2).
375 Yet, the present study suggests that another major alkenone producer at this site was
376 *Cyclicargolithus*, which had an overall larger cell diameter than the reticulofenestrids (Figure
377 6a). We have thus re-evaluated the interpretation of published $\varepsilon_{p37:2}$ values [Figure 6b; *Pagani*
378 *et al.*, 2000b] and re-estimated paleo-pCO_2 values considering the mean cell size of
379 *Cyclicargolithus*. Prior to 20 Ma, this results in higher pCO_2 estimates (max. 340-550 ppmv)
380 compared to values presented in *Henderiks and Pagani* [2007] due to the relatively high
381 proportions and larger size of *Cyclicargolithus*. After 20 Ma, *Cyclicargolithus* is less common
382 than large reticulofenestrids, resulting in pCO_2 estimates (<400 ppmv) that are similar to those
383 determined by *Henderiks and Pagani* [2007]. Overall, the new pCO_2 estimates stay within the
384 ranges previously reported by *Pagani et al.* [2000b] (Figure 6c).
385
386 Relative differences in growth rates between reticulofenestrids and *Cyclicargolithus* can be
387 evaluated using the following model [*Henderiks and Pagani*, 2007]:
388 $$\mu / [CO_{2(aq)}] = (\varepsilon_{p37:2} - \varepsilon_f) / K_{V:SA} \quad (3)$$
389 where the term '*b*' from equation (2) is now expressed by specific growth rate (μ) and a
390 constant ($K_{V:SA}$) that is defined by the cell volume to surface area ratio (V:SA) of eukaryotic
391 species [*Popp et al.*, 1998]:
392 $$K_{V:SA} = 49 - 222(V:SA) \quad (4)$$
393 Under constant $[CO_{2(aq)}]$, and assuming no vital effects in $\varepsilon_{p37:2}$ between different
394 haptophytes, similar values of $\varepsilon_{p37:2}$ could be generated by large cells (high V:SA) with low
395 growth rates and/or small cells with high growth rates (Figure 7). In this scenario, our
396 reconstructions indicate that *Cyclicargolithus* had 30 to 60% lower specific growth rates than
397 the reticulofenestrids.

Without access to cell geometry data and detailed nannofossil data, *Pagani et al.* [2000b] initially calculated an overall ~60% increase in haptophyte growth rates to explain the distinct 6‰ decrease in $\varepsilon_{p37:2}$ observed after ~20 Ma (Figure 6b). Here we combine the *Cyclicargolithus* and reticulofenestrid data (based on their mean size and respective proportions relative to the total Noelaerhabdaceae abundance), and show that the 6‰ shift in $\varepsilon_{p37:2}$ is supported by an increase (~23%) in mean cell size (V:SA) and by an overall increase in mean growth rates of ~24% (Figure 7). The distinct 6‰ shift in $\varepsilon_{p37:2}$ may thus be partly explained by changes in the major alkenone producers with different growth rates under similar CO_2 conditions: from assemblages dominated by slow-growing *Cyclicargolithus* to dominantly reticulofenestrids with higher growth rates. Pairwise correlations (Table 2) show that there is a significant correlation between $\delta^{13}C_{37:2}$ (and therefore $\varepsilon_{p37:2}$) and reticulofenestrid mean size ($R= 0.68$, $p<0.001$); $\delta^{13}C_{37:2}$ and *Cyclicargolithus* mean size ($R=0.69$, $p=0.0002$); and $\delta^{13}C_{37:2}$ and the *Cyclicargolithus*/Noelaerhabdaceae abundance ratio ($R=-0.67$, $p=0.0003$). Finally, the observed variability in alkenone $\delta^{13}C_{37:2}$ and $\varepsilon_{p37:2}$ are best explained by a multiple linear regression linking the $\delta^{13}C_{37:2}$ to changes in mean Noelaerhabdaceae cell size and in the *Cyclicargolithus*/Noelaerhabdaceae abundance ratio ($R=0.81$; $p<0.0001$).

6. Conclusion

A comparison of nannofossil and alkenone absolute contents in Atlantic sediment samples (DSDP Site 516) spanning the late Oligocene to early Miocene suggests that the species *Cyclicargolithus floridanus* was a major alkenone producer between 25 and 20.5 Ma, explaining at least 40% of the total alkenone content at this site. The contribution to alkenone production by large *Dictyococcites* is supported in younger sediments whereas that of *Reticulofenestra* species appears less pronounced. These observations challenge previous

423 statements that *Reticulofenestra* was the most important alkenone producer during the late
424 Oligocene-early Miocene. The relatively high proportions of *Cyclicargolithus* before 20 Ma
425 and its larger cell size lead to higher paleo-pCO_2 estimates than those previously determined
426 without considering this genus. Finally, the variability in alkenone $\delta^{13}C_{37:2}$ and $\varepsilon_{p37:2}$ are
427 explained by changes in mean cell size as well as changes in the major alkenone producers
428 with different growth rates. This highlights the importance of a careful evaluation of the most
429 likely alkenone producers before using alkenone-based proxies for paleoenvironmental
430 reconstructions.
431
432 **7. Appendix A: Taxonomic remarks**
433 Taxonomy used in the present work follows Haptophyte phylogeny as revised by *Young*
434 *and Bown* [1997] and *Sáez et al.* [2004].
435
436 **7.1. Species belonging to the Noelaerhabdaceae Family**
437
438 **7.1.1. Family *Noelaerhabdaceae* Jerkovic 1970 emend. Young & Bown 1997**
439 This is the dominant Family in most Neogene assemblages, considered as the Cenozoic
440 ancestor of the modern alkenone producers *Emiliania* and *Gephyrocapsa*.
441
442 7.1.1.1. Genus *Reticulofenestra* Hay, Mohler and Wade 1966
443 Elliptical to sub-circular coccoliths with a prominent open central area and with no slits in
444 the distal shield. The rather simple morphology of *Reticulofenestra* makes subdivision into
445 species notoriously problematic. The conventional taxonomy is primarily based on size. This
446 is unsatisfactorily and arbitrary, but of stratigraphic value [*Backman*, 1980; *Young et al.*,

2003]. In this study, a subdivision of four size-defined species was employed during the assemblage counts:

Reticulofenestra haqii Backman 1978: morphospecies 3-5 µm in length, with a central opening shorter than 1.5 µm.

Reticulofenestra minuta Roth 1970: morphospecies smaller than 3 µm.

Reticulofenestra minutula (Gartner, 1967) Haq and Berggren, 1978: morphospecies 3-5 µm in length with a central opening longer than 1.5 µm.

Reticulofenestra pseudoumbilicus (Gartner 1967) Gartner 1969: larger morphospecies (5-7 µm).

7.1.1.2. Genus *Dictyococcites* (Black 1967) emend. Backman 1980

Elliptical coccoliths with a large central area closed (or virtually closed) in line with the distal shield. The central area of the distal shield frequently shows a median furrow or a minute pore, but not large enough to suggest that they belong to *Reticulofenestra*. Although *Dictyococcites sensu Black* [1967] can be regarded as a heavily calcified, junior synonym of *Reticulofenestra*, the emended diagnosis of *Backman* [1980] clearly separates this genus from *Reticulofenestra*.

Dictyococcites spp.: small morphospecies (< 3 µm) with a supposed closed central area.

Dictyococcites antarcticus Haq 1976: in contrast with *D. hesslandii*, the specimens of *D. antarcticus* (4-8 µm) show no pore but a narrow and elongated rectangular central area (named "furrow" in *Haq*, 1976 and "straight band" in *Backman*, 1980). The straight extinction band along the major axis occupies at least one half of the total length of the elliptical central area [*Backman*, 1980].

Dictyococcites hesslandii (Haq 1966) Haq and Lohmann, 1976: the central area of the distal shield exhibits a small pore, from which extinction bands radiate (3-8 μm). Two morphometric size classes were distinguished in this study (3-5 μm and >5 μm).

7.1.1.3. Genus *Cyclicargolithus* Bukry 1971

Circular to sub-circular coccoliths with a small central area and high tube-cycles. Although *Theodoridis* [1984] assigned *Cyclicargolithus* as a junior synonym of *Reticulofenestra*, the emended diagnosis of *Bukry* [1971] clearly separates this genus from *Reticulofenestra*.

Cyclicargolithus abisectus (Müller 1970) Wise 1973: large species (>10 μm).

Cyclicargolithus floridanus (Roth and Hay in Hay et al., 1967) Bukry 1971: species smaller than 10 μm.

7.2. Other coccoliths

Calcidiscus leptoporus (Murray and Blackman, 1898) Loeblich and Tappan, 1978

Coccolithus miopelagicus Bukry, 1971

Coccolithus pelagicus (Wallich 1877) Schiller 1930

Helicosphaera spp. Kamptner 1954

Pontosphaera spp. Lohmann 1902

Syracosphaera pulchra Lohmann 1902

Umbilicosphaera spp. Lohmann 1902

7.3. Nannoliths

Discoaster spp. Tan, 1927

Sphenolithus spp. Deflandre in Grassé 1952

Acknowledgements

We would like to thank two anonymous reviewers for their constructive comments and critical review. This study used Deep Sea Drilling Project samples provided by the Integrated Ocean Drilling Program. We thank Walter Hale from the Bremen Core Repository for his efficiency.

References

Armstrong, R.A., C. Lee, J.I. Hedges, S. Honjo, and S.G. Wakeham (2002), A new mechanistic model for organic carbon fluxes in the ocean based on the quantitative association of POC with ballast minerals, *Deep-Sea Res., Part II*, *49*, 219–236.

Aubry, M.P. (1992), Paleogene calcareous nannofossils from the Kerguelen Plateau, Leg 120, in *Proceedings of the Ocean Drilling Program, Scientific Results, College Station, TX (Ocean Drilling Program),* vol. 120**,** edited by S.W. Wise et al., pp. 471-491, doi:10.2973/odp.proc.sr.120.149.

Backman, J. (1980), Miocene-Pliocene nannofossils and sedimentation rates in the Hatton-Rockall basin, NE Atlantic Ocean, *Stockholm Contrib. Geol.*, *36* (1), 1-91.

Bard E., F. Rostek, and C. Sonzogni (1997), Interhemispheric synchrony of the last deglaciation inferred from alkenone paleothermometry, *Nature*, *385*, 707-710, doi:10.1038/385707a0.

Barker, P.F. (1983), Tectonic evolution and subsidence history of the Rio Grande Rise, *Initial Rep. Deep Sea Drill. Proj.*, *72*, 953– 976, doi:10.2973/dsdp.proc.72.151.

Barker P.F., R.L. Carlson, D.A. Johnson and the Shipboard Scientific Party (1983), Site 516: Rio Grande Rise, *Initial Rep. Deep Sea Drill. Proj.*, *72*, 155-338, doi:10.2973/dsdp.proc.72.105.

522 Beaufort, L. (1991a), Dynamique du nannoplancton calcaire au cours du Néogène :
523 Implication climatiques et océanographiques, *M.S. thesis*, Laboratoire de Géologie de
524 Lyon, University Lyon I, 173 pp.
525 Beaufort, L. (1991b), Adaptation of the random settling method for quantitative studies of
526 calcareous nannofossils, *Micropaleontology*, *37*, 415–418.
527 Beaufort, L. (1992), Size variations in Late Miocene *Reticulofenestra* and implication for
528 paleoclimatic interpretation, *Mem. Sci. Geol.*, *43*, 339–350.
529 Belkin, I.M., and A.L. Gordon (1996), Southern Ocean fronts from the Greenwich meridian to
530 Tasmania, *J. Geophyis. Res.*, *101*, 3675– 3696.
531 Beltran, C., J.-A. Flores, M.-A. Sicre, F. Baudin, M. Renard, and M. de Rafélis (2011), Long
532 chain alkenones in the Early Pliocene Sicilian sediments (Trubi Formation – Punta di
533 Maiata section): Implications for the alkenone paleothermometry, *Palaeogeogr.*
534 *Palaeoclimatol. Palaeoecol.*, *308*, 253–263.
535 Bidigare, R.R., A. Fluegge, K.H. Freeman, K.L. Hanson, J.M. Hayes, D. Hollander, J.P.
536 Jasper, L.L. King, E.A. Laws, J. Milder, F.J. Millero, R. Pancost, B.N. Popp, P.A.
537 Steinberg, and S.G. Wakeham (1997), Consistent fractionation of ^{13}C in nature and in the
538 laboratory: Growth-rate effects in some haptophyte algae, *Global Biogeochem. Cycles*, *11*,
539 279–292 (Correction, *Global Biogeochem. Cycles*, *13*, 251– 252, 1999).
540 Bolton, C.T., K.T., Lawrence, S.J. Gibbs, P.A. Wilson, L.C. Cleaveland, D. Timothy, and
541 T.D. Herbert (2010), Glacial-interglacial productivity changes recorded by alkenones and
542 microfossils in late Pliocene eastern equatorial Pacific and Atlantic upwelling zones,
543 *Earth Planet. Sci. Lett.*, *295*, 401-411.
544 Brassell, S.C., G. Eglinton, I.T. Marlowe, U. Pflaumann, and M. Sarnthein (1986), Molecular
545 stratigraphy: a new tool for climatic assessment, *Nature*, *320*, 129-133.

546 Brassell, S.C., M. Dumitrescu, and the ODP Leg 198 Shipboard Scientific Party (2004),
547 Recognition of alkenones in a lower Aptian porcellanite from the west-central Pacific,
548 *Org. Geochem.*, *35*, 181-188.
549 Bukry, D. (1971), Cenozoic calcareous nannofossils from the Pacific Ocean, *Trans. San*
550 *Diego Soc. Nat. Hist.*, *16*, 303-327.
551 Cacho, I., J.O. Grimalt, C. Pelejero, M. Canals, F.J. Sierro, J.A. Flores, and N.J. Shackleton
552 (1999), Dansgaard–Oeschger and Heinrich event imprints in Alboran Sea
553 paleotemperatures, *Paleoceanography*, *14*, 698–705.
554 Conte, M.H., A. Thompson, and G. Eglinton (1995), Lipid biomarker diversity in the
555 coccolithophorid *Emiliania huxleyi* (Prymnesiophycea) and the related species
556 *Gephyrocapsa oceanica*, *J. Phycol.*, *31*, 272–82.
557 Conte, M.H., A. Thompson, D. Lesley, and R.P. Harris (1998), Genetic and physiological
558 influences on the alkenone/alkenoate versus growth temperature relationship in *Emiliania*
559 *huxleyi* and *Gephyrocapsa oceanica*, *Geochim. Cosmochim. Acta*, *62* (1), 51-68.
560 Eglinton, G., S.A. Bradshaw, A. Rosell, M. Sarnthein, U. Pflaumann, and R. Tiedemann
561 (1992), Molecular record of secular sea surface temperature changes on 100-year time-
562 scales for glacial terminations I, II and IV, *Nature*, *356*, 432–426.
563 Eltgroth, M.L., R.L. Watwood, and G.V. Wolfe (2005), Production and cellular localisation of
564 neutral long chain lipids in the Haptophyte algae *Isochrysis galbana* and *Emiliania*
565 *huxleyi*, *J. Phycol.*, *41*, 1000-1009.
566 Ennyu, A., M.A. Arthur, and M. Pagani (2002), Fine-fraction carbonate stable isotopes as
567 indicators of seasonal shallow mixed-layer paleohydrography, *Mar. Micropaleontol.*, *46*,
568 317-342.
569 Epstein, B.L., S. D'Hondt, J.G. Quinn, J. Zhang, and P.E. Hargraves (1998), An effect of
570 dissolved nutrient concentrations on alkenone-based temperature estimates,

571 *Paleoceanography*, *13* (2), 122-126.
572 Farrimond, P., G. Eglinton, and S.C. Brassell (1986), Alkenones in Cretaceous black shales,
573 Blake-Bahama Basin, western North Atlantic, *Org. Geochem.*, *10*, 897-903.
574 Geisen, M., J. Bollmann, J.O. Herrle, J. Mutterlose, and J.R. Young (1999), Calibration of the
575 random settling technique for calculation of absolute abundance of calcareous
576 nannoplankton, *Micropaleontology*, *45* (4), 437-442.
577 Gibbs, S., N. Shackleton, and J.R. Young (2004), Identification of dissolution patterns in
578 nannofossil assemblages: a high-resolution comparison of synchronous records from
579 Ceara Rise, ODP Leg 154, *Paleoceanography*, *19*, PA1029.
580 Gong, C., and D.J. Hollander (1997), Differential contribution of bacteria to sedimentary
581 organic matter in oxic and anoxic environments, Santa Monica Basin, California, *Org.*
582 *Geochem.*, *26*, 545-563.
583 Gong, C., and D.J. Hollander (1999), Evidence for the differential degradation of alkenones
584 under contrasting bottom water oxygen conditions: Implication for paleotemperature
585 reconstruction, *Geochim. Cosmochim. Acta*, *63*, 405-411.
586 Grimalt, J.O., J. Rullkötter, M.-A. Sicre, R. Summons, J. Farrington, H.R. Harvey, M. Goñi,
587 and K. Sawada (2000), Modifications of the C_{37} alkenone and alkenoate composition in
588 the water column and sediment: Possible implications for sea surface temperature
589 estimates in paleoceanography, *Geochem. Geophys. Geosyst.*, 2000GC000053.
590 Hay, W.W., H. Mohler, and M.E. Wade (1966), Calcareous nannofossils from Nal chik
591 (northwest Caucasus), *Eclogae Geol. Helv.*, *56*, 379–399.
592 Henderiks, J. (2008), Coccolithophore size rules - reconstructing ancient cell geometry and
593 cellular calcite quota from fossil coccoliths, *Mar. Micropaleontol.*, *67*, 143-154.

Henderiks, J., and M. Pagani (2007), Refining ancient carbon dioxide estimates: significance of coccolithophore cell size for alkenone-based pCO_2 records, *Paleoceanography*, *22*, PA3202, doi:10.1029/2006PA001399.

Henderiks, J., and A. Törner (2006), Reproducibility of coccolith morphometry: Evaluation of spraying and smear slide preparation techniques, *Mar. Micropaleontol.*, *58*, 207-218.

Jasper, J.P., and J.M. Hayes (1990), A carbon isotope record of CO_2 levels during the late Quaternary, *Nature*, *347*, 462-464.

Jasper, J.P., J.M. Hayes, A.C. Mix, and F.G. Prahl (1994), Photosynthetic fractionation of ^{13}C and concentrations of dissolved CO_2 in the central equatorial Pacific during the last 255000 years, *Paleoceanography*, *9*, 781-798.

Klaas, C., and D.E. Archer (2002), Association of sinking organic matter with various types of mineral ballast in the deep sea: implications for the rain ratio, *Global Biogeochem. Cycles*, *16*, 1116, doi:10.1029/2001GB001765.

Laws, E.A., B.N. Popp, R.R. Bidigare, M.C. Kennicutt, and S.A. Macko (1995), Dependence of phytoplankton carbon isotopic composition on growth rate and $[CO_2]_{aq}$: theoretical considerations and experimental results, *Geochim. Cosmochim. Acta*, *59,* 1131–1138.

Marlowe, I.T., S.C. Brassell, G. Eglinton, and J.C. Green (1984), Long chain unsatured kenones and esters in living algae and marine sediments, *Org. Geochem.*, *6*, 135-141.

Marlowe, I.T., S.C. Brassell, G. Eglinton, and J.C. Green (1990), Long-chain alkenones and alkyl alkenoates and the fossil coccolith record of marine sediments, *Chem. Geol.*, *88*, 349-375.

Martrat, B., J.O. Grimalt, C. Lopez-Martinez, I. Cacho, F.J. Sierro, J.A. Flores, R. Zahn, M. Canals, J.H. Curtis, and D.A. Hodell (2004), Abrupt temperature changes in the western Mediterranean over the past 250,000 years, *Science*, *306*, 1762–1765.

618 Mukhopadhyay, P.K., J. Rullkötter, and D.H. Welte (1983), Facies and diagenesis of organic
619 matter in sediments from the Brazil basin and the Rio Grande Rise, deep Sea Drilling
620 Project Leg 72, *Initial Rep. Deep Sea Drill. Proj.*, *72*, 821-828,
621 doi:10.2973/dsdp.proc.72.138.
622 Müller, P.J., M. Cepek, G. Ruhland, and R.R. Schneider (1997), Alkenone and
623 coccolithophorid species changes in Late Quaternary sediments from the Walvis Ridge:
624 Implications for the alkenone paleotemperature method, *Palaeogeogr. Palaeoclimatol.*
625 *Palaeoecol.*, *135*, 71–96.
626 Müller, P.J., G. Kirst, G. Rulhand, I. von Storch, and A. Rosell-Melé (1998), Calibration of
627 the alkenone paleotemperature index $U^{K'}_{37}$ based on core-tops from the eastern South
628 Atlantic and the global ocean (60°N-60°S), *Geochim. Cosmochim. Acta*, *62* (10), 1757-
629 1772.
630 Pagani, M. (2002), The alkenone-CO_2 proxy and ancient atmospheric CO_2, in *Understanding*
631 *climate change: Proxies, chronology, and ocean-atmosphere interactions*, edited by D.R.
632 Grocke and M. Kucera, *Phil. Trans. R. Soc. Lond. A*, vol. 360, pp. 609-632.
633 Pagani, M., M.A. Arthur, and K.H. Freeman (1999), Miocene evolution of atmospheric
634 carbon dioxide, *Paleoceanography*, *14* (3), 273–292.
635 Pagani, M., K.H. Freeman, and M.A. Arthur (2000a), Isotope analyses of molecular and total
636 organic carbon from Miocene sediments, *Geochim. Cosmochim. Acta*, *64*, 37-49.
637 Pagani, M., M.A. Arthur, and K.H. Freeman (2000b), Variations in Miocene phytoplankton
638 growth rates in the southwest Atlantic: Evidence for Changes in Ocean Circulation,
639 *Paleoceanography*, *15*, 486-496.
640 Pagani, M., J.C. Zachos, K.H. Freeman, B. Tripple, and S. Bohaty (2005), Marked decline in
641 atmospheric carbon dioxide concentrations during the Paleogene, *Science*, *309*, 600– 603.

642 Pahnke, K., and J.P. Sachs (2006), Sea surface temperatures of southern midlatitudes 0-160
643 kyr B.P, *Paleoceanography*, *21*, PA2003, doi:10.1029/2005PA001191.
644 Popp, B.N., E.A. Laws, R.R. Bidigare, J.E. Dore, K.L. Hanson, and S.G. Wakeham (1998),
645 Effect of phytoplankton cell geometry on carbon isotopic fractionation, *Geochim.*
646 *Cosmochim. Acta*, *62*, 69– 77.
647 Prahl, F.G., and S.G. Wakeham (1987), Calibration of unsaturation patterns in long-chain
648 ketone compositions for paleotemperature assessment, *Nature*, *330*, 367-369.
649 Prahl, F.G., G.V. Wolfe, and M.A. Sparrow (2003), Physiological impacts on alkenone
650 paleothermometry, *Paleoceanography*, *18*(2), doi:10.1029/2002PA000803.
651 Pujos-Lamy, A. (1977), Essai d'établissement d'une biostratigraphie du nannoplancton
652 calcaire dans le Pleistocène de l'Atlantique Nord-oriental, *Boreas*, *6*, 323-331.
653 Riebesell, U., A.T. Revill, D.G. Hodsworth, and J.K. Volkman (2000), The effects of varying
654 CO_2 concentration on lipid composition and carbon isotope fractionation in *Emiliania*
655 *huxleyi*, *Geochim. Cosmochim. Acta*, *64*, 4179-4192.
656 Rontani, J.F., and S.G. Wakeham (2008), Alteration of alkenone unsaturation ratio with depth
657 in the Black Sea: Potential roles of stereomutation and aerobic biodegradation, *Org.*
658 *Geochem.*, *39* (9), 1259–1268.
659 Roth, P.H., and W.T. Coulbourn (1982), Floral and solution patterns of coccoliths in surface
660 sediments of the North Pacific, *Mar. Micropaleontol.*, *7*, 1–52.
661 Sáez, A.G., I. Probert, J.R. Young, B. Edvardsen, W. Eikrem, and L.K. Medlin (2004), A
662 review of the phylogeny of the Haptophyta, in *Coccolithophores: From molecular*
663 *processes to global impact*, edited by H.R. Thierstein and J.R. Young, J.R., pp. 251–269,
664 Springer-Verlag, Berlin Heidelberg.
665 Seki, O., G.L. Foster, D.N. Schmidt, A. Mackensen, K. Kawamura, and R.D. Pancost (2010),
666 Alkenone and boron-based Pliocene pCO_2 records, *Earth Planet. Sci. Lett.*, *292*, 201-211.

667 Sun, M.Y., and S.G. Wakeham (1994), Molecular evidence for degradation and preservation
668 of organic matter in the anoxic Black Sea Basin, *Geochim. Cosmochim. Acta*, *58*, 3395-
669 3406.
670 Theodoridis, S. (1984), Calcareous nannofossil biozonation of the Miocene and revision of
671 the helicoliths and discoasters, *Utrecht Micropaleontol. Bull.*, *32*, 1-271.
672 Thierstein, H.R., K.R. Geitzenauer, B. Molfino, and N.J. Shackleton (1977), Global
673 synchroneity of late Quaternary coccolith datum levels: Validation by oxygen isotopes,
674 *Geology*, *5*, 400-404.
675 Volkman, J.K., G. Eglinton, E.D.S. Corner, and T.E.V. Forsberg (1980), Long-chain alkenes
676 and alkenones in the marine coccolithphorid *Emiliania huxleyi*, *Phytochemistry*, *19*,
677 2619-2622.
678 Volkman, J.K., S.M. Barrett, S.I. Blackburn, and E.L. Sikes (1995), Alkenones in
679 *Gephyrocapsa oceanica*: Implications for studies of paleoclimate, *Geochim. Cosmochim.*
680 *Acta*, *59*, 513–520.
681 Weaver, P.P.E., M.R. Chapman, G. Eglinton, M. Zhao, D. Rutledge, and G. Read (1999),
682 Combined coccolith, foraminiferal, and biomarker reconstruction of paleoceanographic
683 conditions over the past 120 kyr in the northern North Atlantic (59°N, 23°W),
684 *Paleoceanography*, *15*, 336-349.
685 Young, J.R. (1990), Size variation of Neogene *Reticulofenestra* coccoliths from Indian Ocean
686 DSDP Cores, *J. Micropaleontol.*, *9*, 71–86.
687 Young, J.R. (1998), Neogene, in *Calcareous Nannofossil Biostratigraphy*, edited by P.R.
688 Bown, pp. 225-265, Chapman and Hall, Cambridge, U.K.
689 Young, J.R., and P.R. Bown (1997), Cenozoic calcareous nannoplankton classification, *J.*
690 *Nannoplankton Res.*, *19*, 36–47.

691 Young, J.R., M. Geisen, and I. Probert (2005), A review of selected aspects of
692 coccolithophore biology with implications for palaeobiodiversity estimation,
693 *Micropaleontology*, *51* (4), 267-288.

694

695 **Figure captions**

696 **Figure 1.** Location of DSDP Site 516 at the Rio Grande Rise [adapted from *Henderiks and*
697 *Pagani*, 2007].

698

699 **Figure 2. (a)** Total organic carbon content (wt% TOC), **(b)** total alkenone content (µg g
700 sediment^{-1}), **(c)** total alkenone content relative to TOC (µg g TOC^{-1}), **(d)** absolute abundance
701 of nannofossils (specimens g sediment^{-1}) and **(e)** absolute abundance of Noelaerhabdaceae
702 (coccoliths g sediment^{-1}) at DSDP Site 516 during the late Oligocene-early Miocene. Error
703 bars represent coefficients of variation.

704

705 **Figure 3.** Comparison between alkenone concentration and Noelaerhabdaceae distribution at
706 DSDP Site 516 during the late Oligocene-early Miocene. **(a)** Total alkenone content (µg g
707 sediment^{-1}); **(b-d)** absolute and relative abundances of **(b)** *Cyclicargolithus,* **(c)** *Dictyococcites*
708 and **(d)** *Reticulofenestra*. Relative abundances are relative to the total nannofossil contents.
709 Trend curves are moving average curves calculated using a 0.5 Ma window size and a 0.25
710 Ma time step. Scale bars on nannofossil pictures equal to 4 µm.

711

712 **Figure 4.** Relative abundances of *Cyclicargolithus* species, *C. floridanus* and *C. abisectus*, at
713 DSDP Site 516. It should be noted that *C. floridanus* is entirely responsible for the
714 *Cyclicargolithus* abundance trend.

715

716 **Figure 5.** Correlations (linear regressions; α=0.05) between alkenone content (µg g sediment^{-1}) and **(a)** relative and **(b)** absolute abundances of *Cyclicargolithus* during the late Oligocene-early Miocene at DSDP Site 516.

719

720 **Figure 6. (a)** Mean size variability at Site 516 of reticulofenestrids (*Reticulofenestra* + *Dictyococcites*) and *Cyclicargolithus*, as determined in the 24 samples studied by *Henderiks and Pagani* [2007] (error bars indicate 95% confidence intervals); **(b)** alkenone-derived $\varepsilon_{p37:2}$ record [from *Pagani et al.*, 2000b]; **(c)** revised pCO_2 estimates after cell size corrections [see detailed methods in *Henderiks and Pagani*, 2007] including *Cyclicargolithus* (in blue) compared to pCO_2 estimates of *Pagani et al.* [2000b] (in grey) and *Henderiks and Pagani* [2007] (in red). Shaded bands/lines depict minimum and maximum estimates with propagated 95% confidence levels of input factors, dashed lines represent minimum estimates assuming no diagenetic alteration of biogenic carbonates used to determine paleo-SST [see *Pagani et al.*, 2005].

730

731 **Figure 7.** Relationship between $\varepsilon_{p37:2}$ (‰), cell volume to surface area ratios (V:SA; µm), and growth rates (μ_{cc}; day^{-1}), calculated with constant $CO_{2(aq)}$ = 10µmol kg^{-1} [after *Henderiks and Pagani*, 2007]. The contoured growth rates represent values under continuous-light chemostat experiments and need to be corrected for the effect of day length and respiration in natural settings [*Bidigare et al.*, 1997]. The star symbols depict the 6‰ decrease in $\varepsilon_{p37:2}$ between 20.3 and 19.5 Ma, which, under constant CO_2, corresponds to an increase in Noelaerhabdaceae cell sizes and growth rates.

738

739 **Table 1**. Distinctive morphological features used to distinguish the three Noelaerhabdaceae
740 genera (*Reticulofenestra, Dictyococcites* and *Cyclicargolithus*) at DSDSP Site 516 during the
741 late Oligocene-early Miocene.
742
743 **Table 2**. Pairwise linear regressions between alkenone $\delta^{13}C$ ($\delta^{13}C_{37:2}$), $\varepsilon_{p37:2}$, *Cyclicargolithus*
744 and reticulofenestrids mean cell size, and the ratio of *Cyclicargolithus* to Noelaerhabdaceae.
745

746

747

Noelaerhabdaceae genus	Distinctive morphological features
Reticulofenestra	Elliptical coccoliths with a prominent open central area and with no slits in the distal shield [*Hay et al.*, 1966].
Dictyococcites	Elliptical coccoliths with a large central area closed or virtually closed in line with the distal shield. The central area of the distal shield frequently shows a median furrow or a minute pore [*Backman*, 1980].
Cyclicargolithus	Circular to sub-circular coccoliths with a small central area and high tube-cycles [*Bukry*, 1971]. Larger coccolith size range than *Reticulofenestra* and *Dictyococcites* [*Henderiks*, 2008].

748 Table 1.

749

750

	$\delta^{13}C_{37:2}$	$\varepsilon_{p37:2}$	**Reticulofenestrid mean size**	***Cyclicargolithus* mean size**	**Mix mean size**
$\varepsilon_{p37:2}$	R= -0.96 *p*<0.0001				
Reticulofenestrid mean size	R= 0.68 *p*=0.0003	R= -0.68 *p*=0.0003			
***Cyclicargolithus* mean size**	R= 0.69 *p*=0.0002	R= -0.67 *p*=0.0004	R= 0.75 *p*<0.0001		
Mix mean size	R= 0.33 *p*=0.112	R= -0.36 *p*=0.085	R= 0.86 *p*<0.0001	R= 0.50 *p*=0.013	
***Cyclicargolithus*/ Noelaerhabdaceae**	R= -0.67 *p*=0.0003	R= 0.62 *p*=0.0013	R= -0.34 *p*=0.099	R= -0.60 *p*=0.002	R= -0.17 *p*=0.419

751 Table 2.

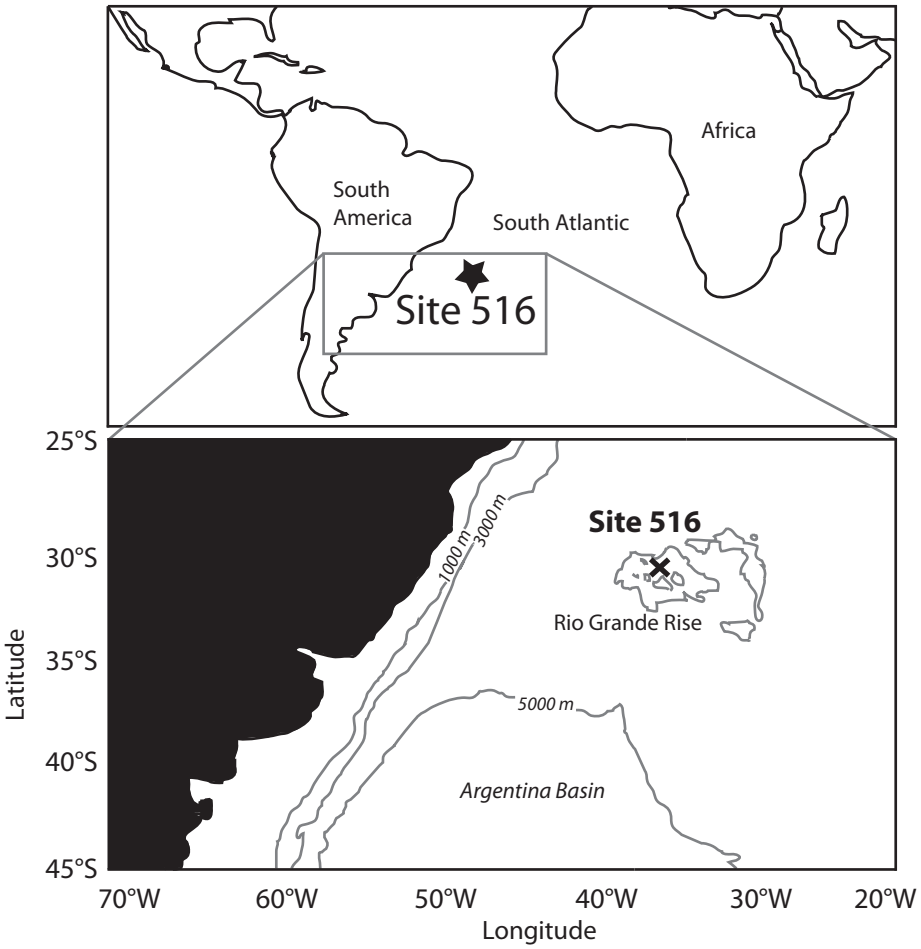
Africa
South America
South Atlantic
Site 516
25°S
30°S
35°S
40°S
45°S
Latitude
1000 m
3000 m
Site 516
Rio Grande Rise
5000 m
Argentina Basin
70°W
60°W
50°W
40°W
30°W
20°W
Longitude

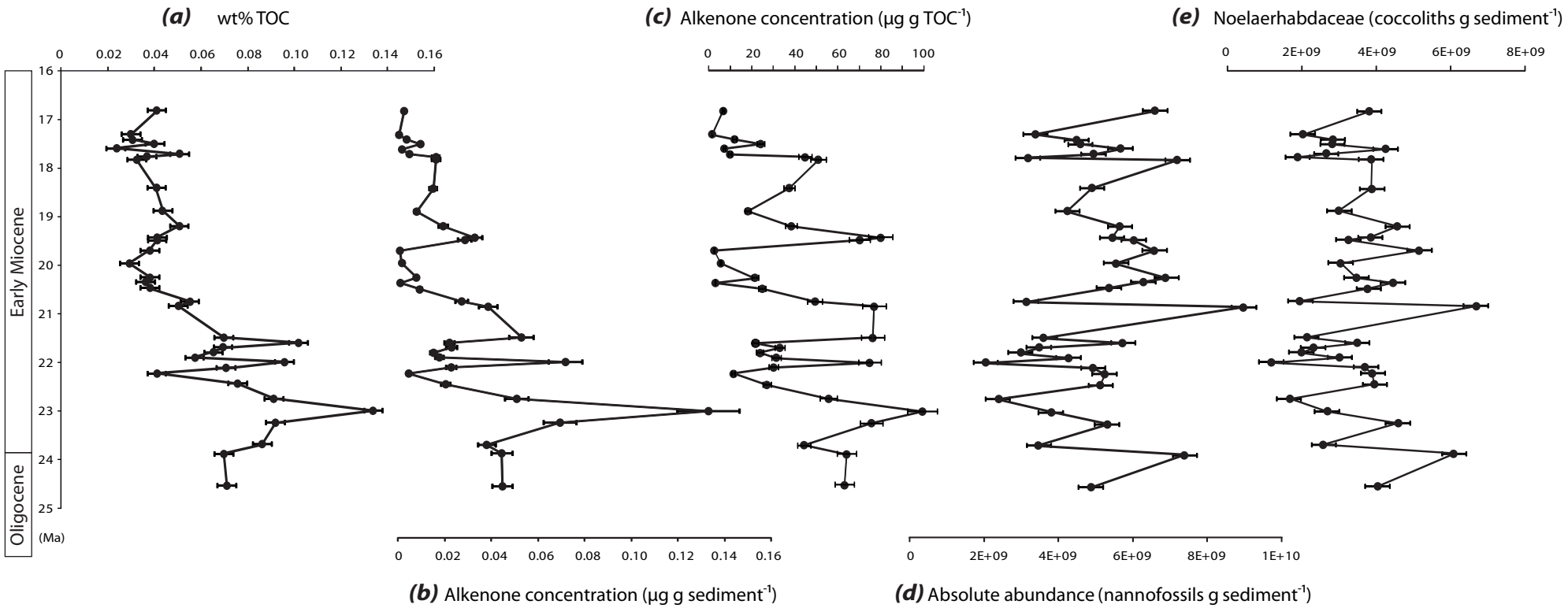
(a) wt% TOC
0 0.02 0.04 0.06 0.08 0.10 0.12 0.14 0.16
(c) Alkenone concentration (µg g TOC-1)
0 20 40 60 80 100
(e) Noelaerhabdaceae (coccoliths g sediment-1)
0 2E+09 4E+09 6E+09 8E+09
Early Miocene
Oligocene
16 17 18 19 20 21 22 23 24 25
(Ma)
0 0.02 0.04 0.06 0.08 0.10 0.12 0.14 0.16
(b) Alkenone concentration (µg g sediment-1)
0 2E+09 4E+09 6E+09 8E+09 1E+10
(d) Absolute abundance (nannofossils g sediment-1)

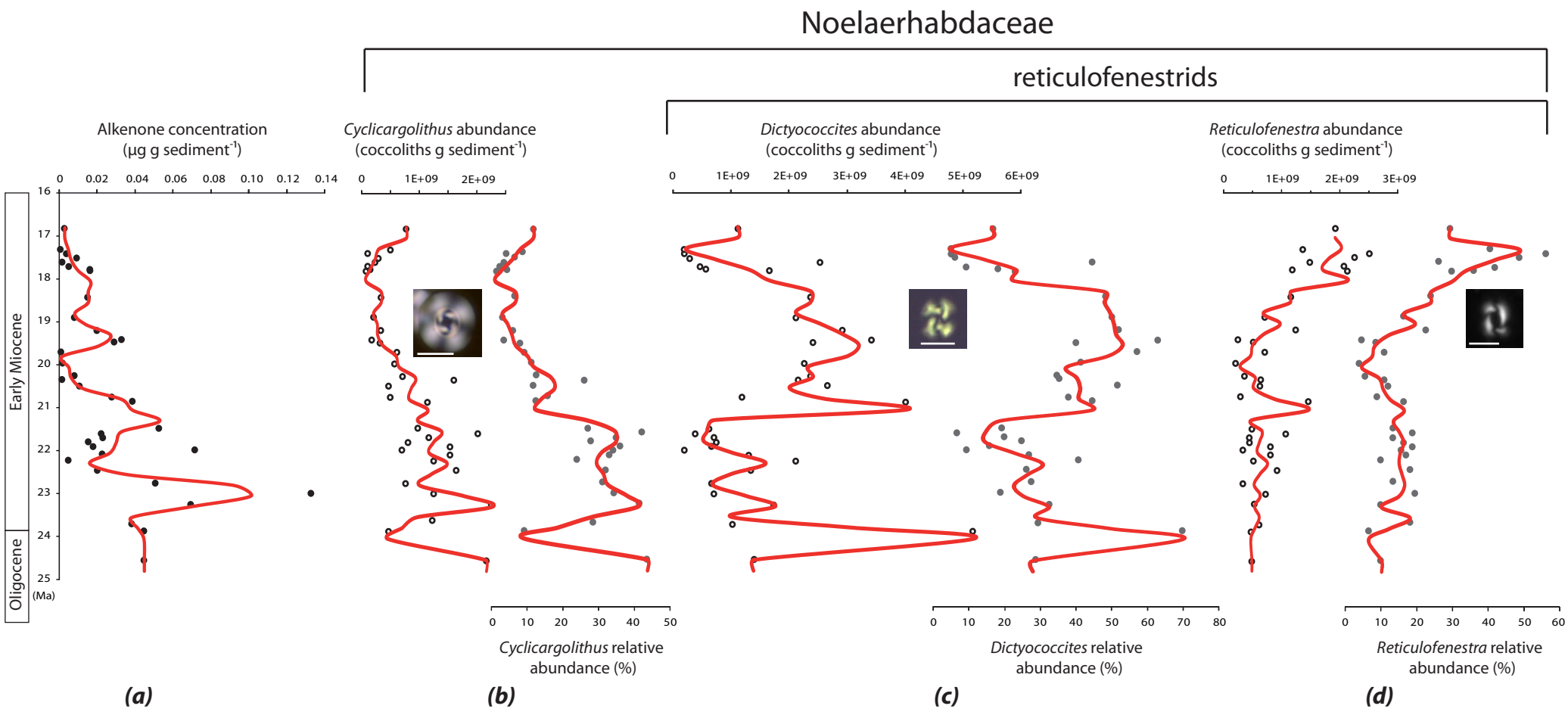
Noelaerhabdaceae
reticulofenestrids
Alkenone concentration (µg g sediment-1)
Cyclicargolithus abundance (coccoliths g sediment-1)
Dictyococcites abundance (coccoliths g sediment-1)
Reticulofenestra abundance (coccoliths g sediment-1)
Early Miocene
Oligocene
(Ma)
Cyclicargolithus relative abundance (%)
Dictyococcites relative abundance (%)
Reticulofenestra relative abundance (%)
(a)
(b)
(c)
(d)

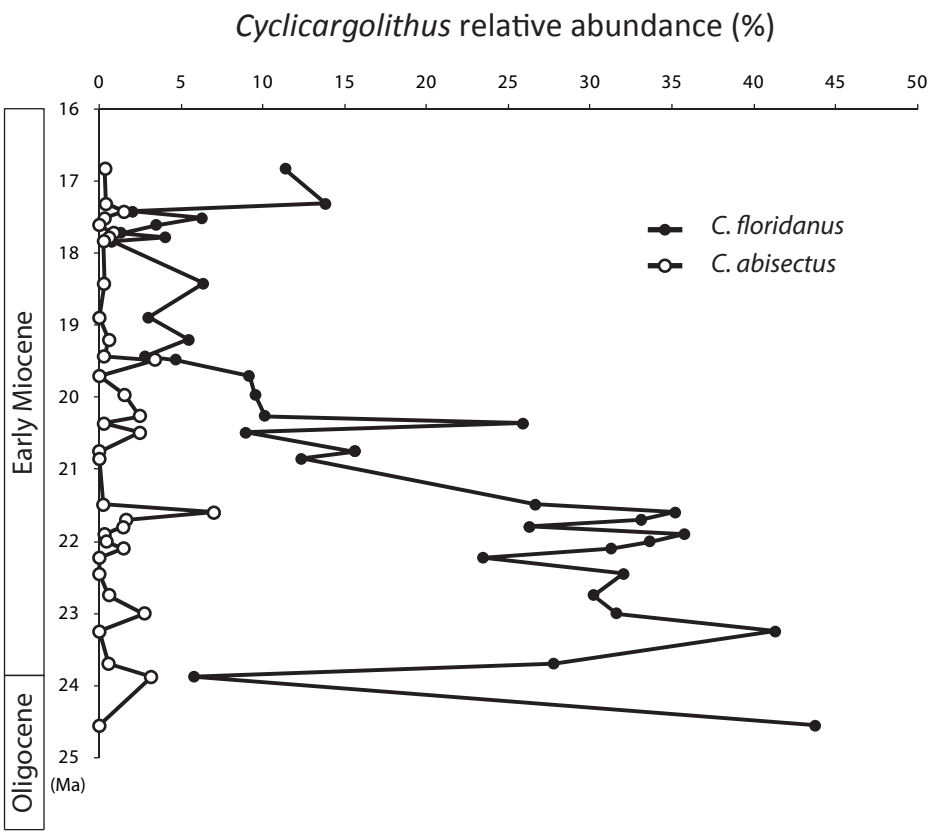
Cyclicargolithus relative abundance (%)
0
5
10
15
20
25
30
35
40
45
50
16
17
18
19
20
21
22
23
24
25
(Ma)
Early Miocene
Oligocene
C. floridanus
C. abisectus

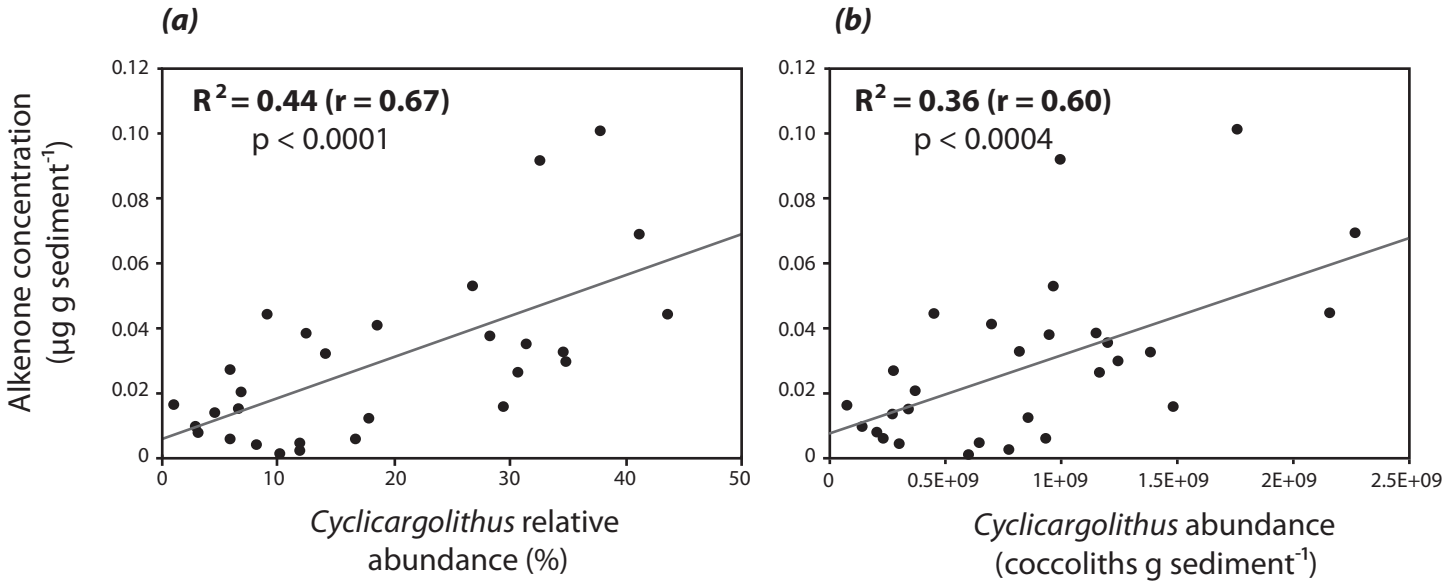
(a)
(b)
Alkenone concentration (µg g sediment-1)
R2 = 0.44 (r = 0.67)
p < 0.0001
R2 = 0.36 (r = 0.60)
p < 0.0004
0.12
0.10
0.08
0.06
0.04
0.02
0
0
10
20
30
40
50
0.5E+09
1E+09
1.5E+09
2E+09
2.5E+09
Cyclicargolithus relative abundance (%)
Cyclicargolithus abundance (coccoliths g sediment-1)

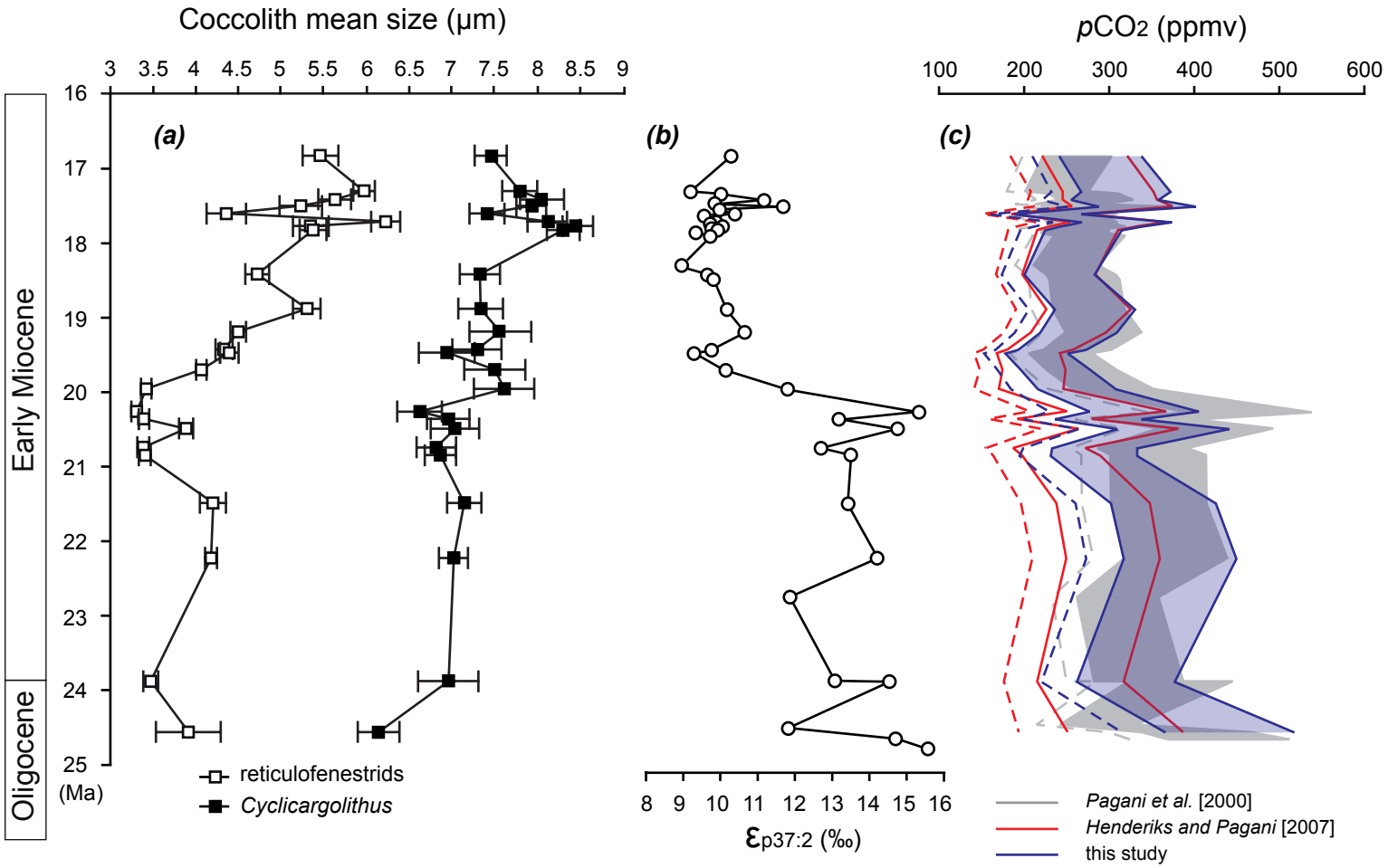
Coccolith mean size (µm)
3 3.5 4 4.5 5 5.5 6 6.5 7 7.5 8 8.5 9
(a)
(b)
(c)
pCO2 (ppmv)
100 200 300 400 500 600
Early Miocene
Oligocene
16 17 18 19 20 21 22 23 24 25
(Ma)
reticulofenestrids
Cyclicargolithus
8 9 10 11 12 13 14 15 16
εp37:2 (‰)
Pagani et al. [2000]
Henderiks and Pagani [2007]
this study

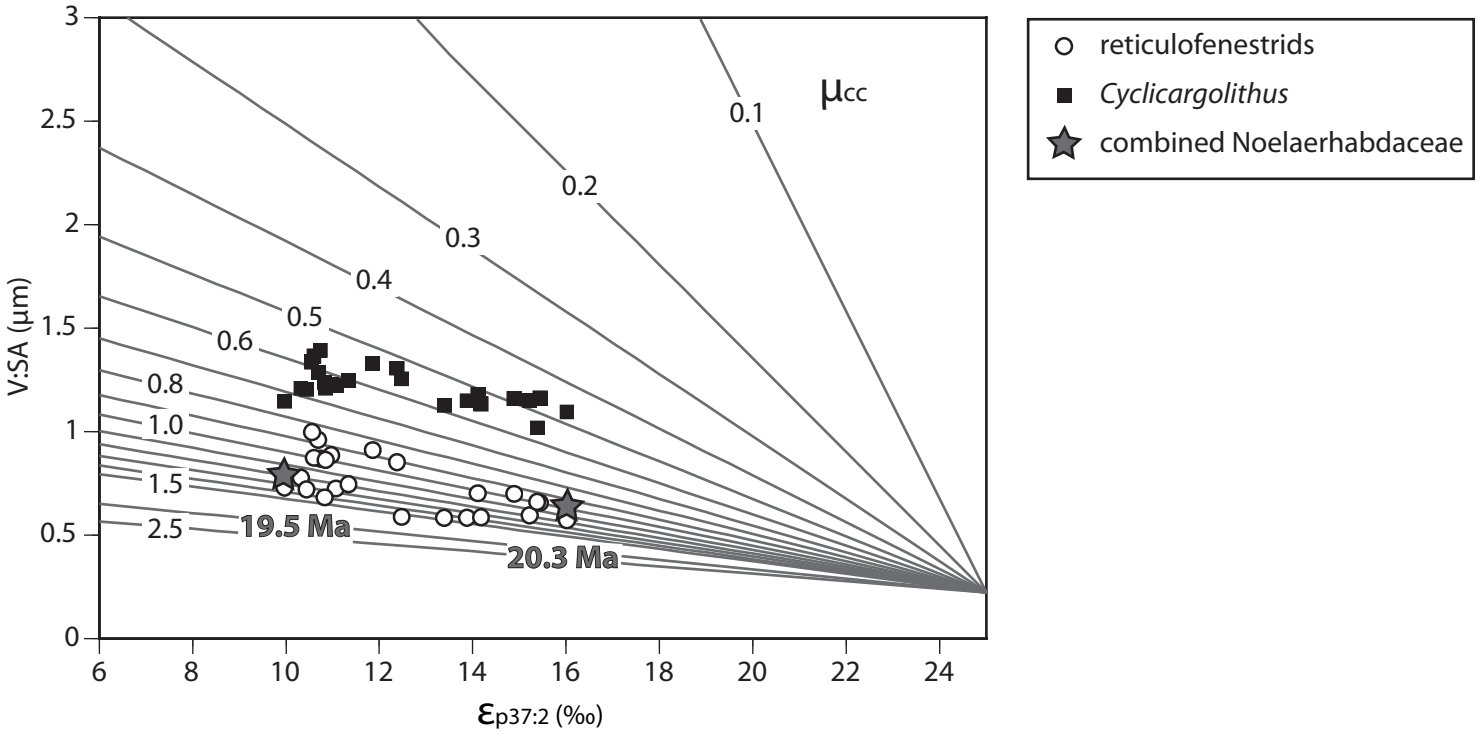
reticulofenestrids
Cyclicargolithus
combined Noelaerhabdaceae
μcc
0.1
0.2
0.3
0.4
0.5
0.6
0.8
1.0
1.5
2.5
19.5 Ma
20.3 Ma
V:SA (μm)
εp37:2 (‰)
0
0.5
1
1.5
2
2.5
3
6
8
10
12
14
16
18
20
22
24